Atomistic Dynamics of Nanoscale Polymer Particles

Kazuhiko Fukui, Bobby G. Sumpter, Michael D. Barnes, and Donald W. Noid*

Chemical and Analytical Sciences Division, Oak Ridge National Laboratory, Oak Ridge, Tennessee 37831-6197

Received January 11, 2000; Revised Manuscript Received May 31, 2000

ABSTRACT: Full classical molecular dynamics was used to study the atomistic details of nanometer scale polymer particles. Using a previously developed efficient molecular dynamics-based method for the generation of polymeric nanoparticles, we model polyethylene (PE) with up to 120 000 atoms, poly(ethylproplyene) (PEP), atactic polypropylene (aPP), and polyisobutylene (PIB) with up to 12 000 backbone atoms. A variety of characteristics and thermodynamical properties of those nanoscale particles are obtained to interpret the properties of a fine polymer particle distinguished from the bulk solid phase. The molecular volume and total energy as a function of temperature are calculated to predict the melting point, glass transition temperature, and heat capacity for the nanoscale particles.

I. Introduction

A recent technology based on microdroplet stream techniques was developed for creating monodisperse polymer particles of arbitrary composition and size from solution.[1−3] This method can be used to produce polymer nano- and microparticles that can be made as small as ∼200 nm with size dispersion of about 1−2%. The refractive index obtained from the data analysis of the particles is consistent with bulk values, and the level of agreement indicates that the particles are nearly perfect spheres. With this technique, homogeneous polymer blend microparticles was also generated from bulk-immiscibe polymer components in solution. For small droplets of solution (<10 μm), the initial volume is sufficiently small that the solvent evaporation time scale is too short for the polymer components to achieve phase equilibrium. Applications of such particles take advantage of high surface area and confinement effects, which lead to nanostructures with different properties than conventional materials.

Computational molecular modeling provides a way of visualizing processes at a sub-macromolecular level that also connects theory and experiment. Particularly attractive from a computational point of view is that the particles are very close to the size scale where a complete atomistic model can be studied without using artificial constraints such as periodic boundary conditions, yet these particles are too small for traditional experimental structure/property determination. Polymeric particles in the nano- and micrometer size range may show many new and interesting properties due to size reduction to the point where critical length scales of physical phenomena become comparable to or larger than the size of the structure itself. This size-scale mediation of the properties (mechanical, physical, electrical, etc.) opens a facile avenue for the production of materials with predesigned properties.[4,5] We have developed a number of novel and powerful computational techniques that allow us to develop a molecular level understanding of how the various properties are influenced by the size scale of the material.[6−8]

The primary tool is a molecular dynamics-based computational algorithm for generating and modeling polymer nanoparticles which leads to particles that are as similar as possible to the experimentally created polymer particles.[7] A great variety of MD simulations have been used for exploring the structural and mechanical properties of a bulk polymer system.[9−13] In contrast, our ongoing research is most interested in the interpretation of the structure and properties of nanoscale polymer particles and how the particles are distinguished from their bulk solid phase. Previously, we have modeled fine polymer particles which should closely correspond to the ones that can be experimentally created from a droplet generator. The structure and a variety of physical characteristics (melting point, glass transition temperature, heat capacity, etc.) have been calculated in order to develop a fundamental understanding of the thermodynamic properties of nanoscale polymer particles. In this paper, we are interested in investigating larger scale PE particles and other polymer particle compositions.

II. Methods

A. Modeling of PE Particles. To obtain initial conditions for polymer particles simulations, we have developed an efficient method described in ref 7. Since we are particularly interested in large-scale MD simulations involving atoms in the range of 3000−120 000 atoms over long time scale, the CH_2 and CH_3 groups were treated as a single particle (monomer) of mass m = 14.5 amu. A classical molecular Hamiltonian for this system can be written in terms of the kinetic T and potential energy V of the system included two-, three-, and four-body bonded interactions in addition to nonbonded terms,

$$H = T + \sum V_{2b}(r_{i,\,i+1}) + \sum V_{3b}(\theta_{i,\,i+1,\,i+2}) + \sum V_{4b}(\tau_{i,\,i+1,\,i+2,\,i+3}) + \sum_{i=1}^{N-3} \sum_{j\geq i+3}^{N} V_{Nb}(r_{ij}) \quad (1)$$

where N is a total number of atoms. The r, q, and t are the internal coordinates for the interatomic distance, the bending angle between three consecutive atoms, and the torsional angle between four consecutive atoms, respectively.

We have developed an efficient molecular dynamics-based method for obtaining a desired size of polymer particles.[7,8] Briefly, the procedure starts by preparing

10.1021/ma000045k CCC: $19.00
Published on Web 07/20/2000

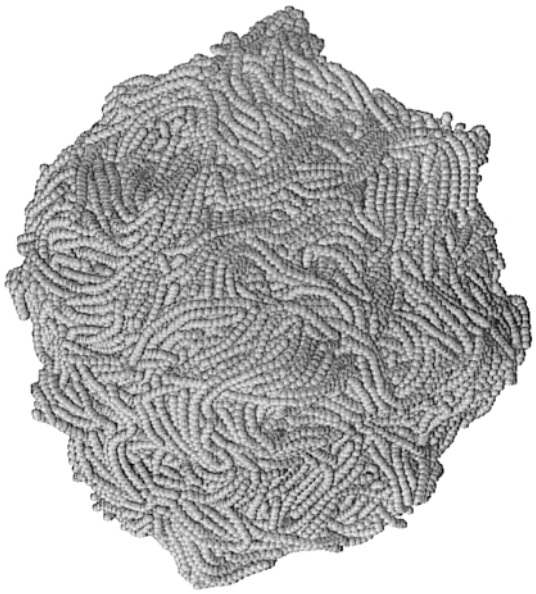

Figure 1. Polyethylene particle of 120 000 atoms with a chain length of 100 monomers. The diameter of the drop is 16.1 nm.

a set of randomly coiled chains with a chosen chain length by propagating a classical trajectory to create a collision at the Cartesian origin. The collision creates a particle consisting of six chains which is annealed to a desired temperature and rotated through a randomly chosen set of angles in three-dimensional space. Another set of six chains are propelled at the particle to create a particle with 600 more atoms. This process is continued until the desired size is reached. This method creates homogeneous particles that are in good agreement with 2-D diffraction observations on experimentally generated polymer particles. Figure 1 shows a 120 000-atom PE particle with a chain length of 100 monomers.

B. Mutation of Polymer Particles. We efficiently generate desired sizes of poly(ethylproplyene) (PEP), atactic polypropylene (aPP), and polyisobutylene (PIB) particles by "mutating" from the configuration of PE particles. To do this, we simply expand the space of the PE particle by multiplying the initial configuration by 1.2 in Cartesian coordinates. Then, a new atom is inserted at a desired position. For example, in the mutation of PEP from PE, 25 new atoms are placed for every PE chain at the position where the distance between a backbone ($4i - 2$) and inserted atom is the −CH2−CH3 equilibrium distance. The potential bonded and nonbonded interactions between the backbone and inserted atoms are adiabatically turned on using a switching function, $SW(t)$. The switching function used for this study is

$$SW(t) = \tanh(9.7786 \times 10^{-3} t) \qquad (2)$$

where t is time (picoseconds). The Hamiltonian for the mutated system can be written

$$H' = H + SW(t)V_{\text{mutate}} \qquad (3)$$

where V_{mutate} is the potential energy functions[14] for the inserted atoms. At a start of the MD simulations for mutated systems, the initial values of the Cartesian momenta are randomly chosen in phase space. Classical trajectories are propagated for 60 ps above the bulk melting point, and then the system is annealed by scaling the Cartesian momenta with a constant scaling factor until the temperature reaches 10 K to find a steady state of the amorphous particles. Using this mutation scheme, various polymer particles can be efficiently modeled. Because the system is annealed to an equilibrium state, the underlying potential energy functions should correctly direct the system toward the correct local and global conformational properties (i.e., characteristic ratio). This can be verified by performing the above proceedure for a bulk simulation. Finally, examination of the conformations and properties at a given temperature was performed using Nosé−Hoover chain (NHC) constant temperature molecular dynamics for the equilibrated (annealed) systems.

We also simulate bulk systems of PE, PEP, aPP, and PIB considering all atoms, to study the structural difference of the particles due to the size reduction and the shape. The computed structural conformations of the bulk systems have very good agreement with X-ray and neutron scattering experiments (e.g., radial distribution).

C. Surface and Thermodynamic Analysis. In analyzing surface effects of ultrafine polymer particles, we calculated the surface area and volume using Connolly's contact-reentrant method.[15] The method provides a smooth surface by patching the space between a probe radius and a probed molecule. For our surface area and volume calculations, the van der Waals radius for the particles is set at 1.89 Å for CH_2 monomers and the probe radius at 1.4 Å to mimic a H_2O molecule.

Calculating temperature, volume, and total energy in the process of annealing the system, we obtain thermodynamic properties (melting point, glass transition temperature, and heat capacity) of nanoscale polymer particles. The melting point T_m and the glass transition temperature T_g can be obtained by calculating total energy E and molecular volume V of a system as a function of temperature. For a transition from the amorphous (solid) to the melt phase (liquid) and a glass−rubber transition, the volume increases owing to conformational disorder of the polymer particles. From least-squares fits to V vs T and E vs T, we take the point where the extrapolated straight lines intersect, as T_g and T_m. The appropriate annealing schedule was determined by examining the melting point and glass transition temperature for 3000 and 12 000 atom PE particles for different rates in the range from 1.7 to 29.5 K/ps. The transition temperatures were found to be rather insensitive (within the error of ±5 K) to annealing rates slower than 6.0 K/ps.[7] In all subsequent simulations, we set the annealing rate at approximately 2.5 K/ps so that the particle is thermally equilibrated for each sampling point.

III. Results and Discussion

A. Characteristics. We have used the molecular dynamics technique to generate PE particles with various chain lengths with up to 120 000 atoms, PEP, aPP, and PIB with up to 12 000 backbone atoms. A fundamental difference between the polymer particles and the bulk system results from surface effects in which the smaller sized particles have more surface area than the larger ones. To investigate the surface effect of the particles, we determined the number surface atoms and obtained the ratio of the surface atoms to the total number of atoms. Figure 2 shows the ratio as a function of diameter. As can be expected, the ratio

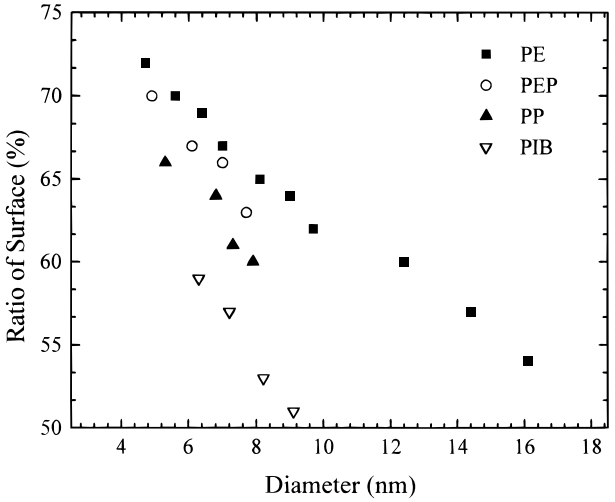

Figure 2. Dependence of ratio of surface atom to total number of atoms for PE, PEP, aPP, and PIB particles.

Table 1. Surface Effects in Ultrafine Polymer Particles

no. of backbone atoms	diam (nm)	ratio of chain ends (%)	area (nm^2)	vol (nm^3)	S_{ration} (nm^{-1})	fractal dimension
			Polyethylene (PE)			
3 000	4.7	95	152	67	2.27	2.14
6 000	5.6	87	257	138	1.86	2.15
9 000	6.4	85	346	209	1.65	2.16
12 000	7.0	83	443	279	1.55	2.16
18 000	8.1	79	610	419	1.46	2.19
24 000	9.0	76	814	564	1.44	2.21
30 000	9.7	71	955	706	1.35	2.21
60 000	12.4	69	1879	1424	1.32	2.26
90 000	14.1	62	2765	2127	1.30	2.28
120 000	16.1	60	4035	3128	1.29	2.28
			Polyethylpropylene (PEP)			
3 000	4.9	85	190	86	2.22	2.19
6 000	6.1	81	327	175	1.87	2.21
9 000	7.0	81	478	264	1.81	2.22
12 000	7.7	74	568	354	1.60	2.25
			Atactic Polypropylene (aPP)			
3 000	5.3	77	235	105	2.24	2.21
6 000	6.8	75	416	214	1.94	2.21
9 000	7.3	74	604	322	1.88	2.24
12 000	7.9	70	780	431	1.81	2.28
			Polyisobutylene (PIB)			
3 000	6.3	75	332	131	2.53	2.25
6 000	7.2	72	683	262	2.60	2.28
9 000	8.2	71	948	399	2.38	2.32
12 000	9.1	68	1193	539	2.21	2.45

decreases when the size of the particles increases. Since the smaller sized particles have more surface atoms than the larger ones, a decrease of the diameter increases the ratio. The large ratio of surface atoms to the total number of atoms leads to a reduction of the nonbonded interactions for the surface layer; hence, the cohesive energy is dramatically dependent on the size. In addition, the ratio of surface chain ends to total number of chain ends for the particles is much larger than that of the bulk system, leading to enrichment of chain ends at surface. This observation is consistent with analysis of thin films.[16−18] With regard to an effect of the side atoms, the increase in the side atoms corresponds to a decrease in the ratio of surface atoms and therefore represents an increase of cohesive energy of the system (see Tables 2 and 3). The increase in cohesive energy is due to the increase in the number of atoms that are inside the spherical particle versus on the surface. This phenomenon is a result of the finite-sized spherical confinement of the particle and is different than what is observed in the corresponding bulk systems (side chains tend to lower the cohesive energy).

Table 2. Thermal Properties of Polyethylene Particles

no. of backbone atoms	cohesive energy[a] (kcal/mol)	T_m (K)	T_g (K)	C_p (cal/(mol K)) $T \le T_m$	C_p (cal/(mol K)) $T \ge T_m$
		Chain Length of 100 Beads			
3 000	3 010	218	111	6.37	7.57
6 000	6 510	234	134	6.50	7.70
9 000	10 170	244	131	6.44	7.22
12 000	13 900	242	157	6.47	7.24
18 000	23 900	249	155	6.44	7.66
24 000	32 000	254	154	6.45	7.95
30 000	41 170	258	152	6.40	7.53
60 000	82 950	266	161	6.65	7.80
90 000	125 240	272	162	6.96	8.25
120 000	166 200	285	170	6.64	8.01
		Chain Length of 50 Beads			
6 000	7 510	186	73	6.20	7.23
12 000	15 300	218	110	6.37	7.74
18 000	25 200	258	131	6.50	7.93
24 000	34 500	272	151	6.54	8.14
		Chain Length of 200 Beads			
6 000	5 738	285	152	6.37	8.02
12 000	10 020	317	162	6.76	7.73
18 000	18 100	330	175	6.80	8.18
24 000	25 300	351	180	6.89	8.15
bulk[b]	9 073	414	195	5.19	7.67

[a] The values are calculated from NHC simulations at 10 K. [b] Cubic boundary conditions were used with a box length of 4.6 nm. The values of C_p are from ref 24 at 300 and 400 K.

To calculate the surface area and volume of the polymer particles, we used the contact-reentrant surface at probe radii $R_p = 1.4$ Å. A proportional surface area S_{ratio}, which is defined by S_{ratio} = (surface area)/(volume), provides the dependence of surface effect on the particle size. The large S_{ratio} leads to large surface free energy, which is defined by per unit of surface area (J/nm^2). The S_{ratio} decreases with an increase of the particle size, and an increase of the number of the side atoms attached on the backbone chains increases the proportional surface area. It suggests that the side chains (CH_3 group) provide cavities (free volume) on the surface of the particles, and the spherical probe penetrates those holes, leading to a large surface area. To characterize the surface of the particles, we examine a fractal dimension which describes a degree of irregularity of a surface.[19] Figure 3 shows dependence of surface area A_s on probe radii R_p for a 12 000 backbone atoms PIB particle. The fractal dimension D determined by the slope can have values in the range 2−3; the lower limit corresponds to a smooth surface and the upper limits to a space-filled surface. The values of D of the particles in a probe range from 2.0 to 3.5 Å are smaller for the particles than the value of the bulk ($D = 2.72$). This indicates that the surface is irregular and has many cavities which may introduce unique (catalytic or interpenetrating) properties of polymer ultrafine particles. This also predicts that nanoscale polymer particles are loosely packed and can show dynamical flexibility. In our previous study,[8] the compressive modulus is investigated for the PE particles by applying an external force in MD simulations. In the study we have observed a compressive modulus that is orders of magnitude smaller than the bulk values. The stress−strain curve actually looks more like a curve for an elastomer. The free volume and molecular packing can be important in a

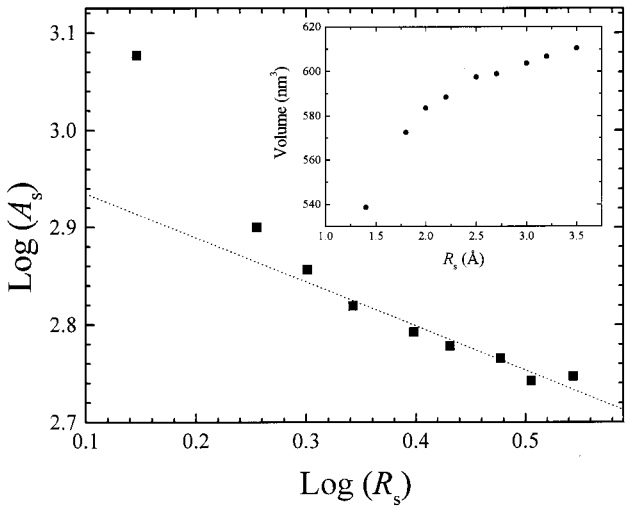

Figure 3. Dependence of molecular surface area, A_s, on probe with radii, R_p, of 1.4−4 Å for a 18 780-atom PIB particle with chain length of 100 beads. The slope of the straight line for log A_s vs log R_p with the least-squares fit is 0.45. The value of fractal dimension is evaluated for probe radii in the range of 2.0−4.0 Å. The inset shows dependence of molecular volume on R_p.

diffusion rate of a small molecule trapped in the particles. The figure also shows the dependence of volume of the PIB particle on probe radii in the range from 1.4 to 3.5 Å. When the radius increases, the volume increases and the surface area decreases. The values of surface area and volume are sensitive to the size of the probe radii. The characteristics of the particles up to 120 000 atoms is summarized in Table 1.

B. Thermal Analysis. Most homogeneous solids have a very specific melting temperature. In order for a particular material to change its state, it must change its thermal energy: to vaporize it requires extra energy; to freeze (fuse), energy must be given up. The latent heat of fusion of a solid is the amount of energy that must be transferred to the solid at its melting point temperature in order to melt it. There is no temperature change associated with this energy transfer, and there is only a change in phase. Our determination of a melting point for the particles is based on the change of energy as a function of temperature (thermodynamic melting). Figure 4a shows dependence of total energy of the system on temperature for the PIB 12 000 backbone atom particle with a chain length of 100 monomers. The slopes provide the constant pressure heat capacity, C_p, above and below the melting point. Figure 4 b shows molecular volume vs temperature. The melting points calculated from molecular volume for the different size of the particles with various chain lengths are close to those values calculated from total energy within an error of ±10 K. We also investigated the melting mechanism of the polymer particles as a function of size, chain length, and temperature.[20] In the simulation, diffusion coefficients of the surface and inner chains of the PE particles were calculated. The results of the simulation show that the mobility of the surface chains is larger than the inner chains (surface melting), and the melting point obtained from the diffusion coefficients as a function of temperature has good agreement with the temperature of thermodynamic melting. Table 2 shows thermal properties of the PE particles with respect to size and various chain lengths. A strong dependence of the melting point and the glass

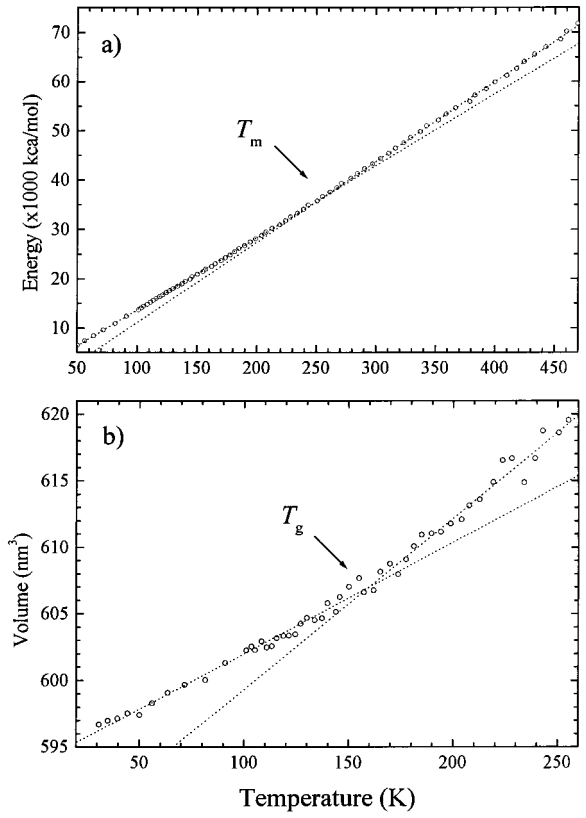

Figure 4. (a) The total energy as a function of temperature while annealing a 18 780-atom PIB particle. The open circles are the total energy calculated from MD simulations, and dashed lines show the least-squares fit. The intersection of extrapolated straight lines corresponds to the melting point, T_m = 258 K. (b) The molecular volume as a function of temperature. The open circles are the volume calculated from MD simulations, and dashed lines show the least-squares fit. The intersection of extrapolated straight lines corresponds to the glass transition temperature, T_g = 160 K.

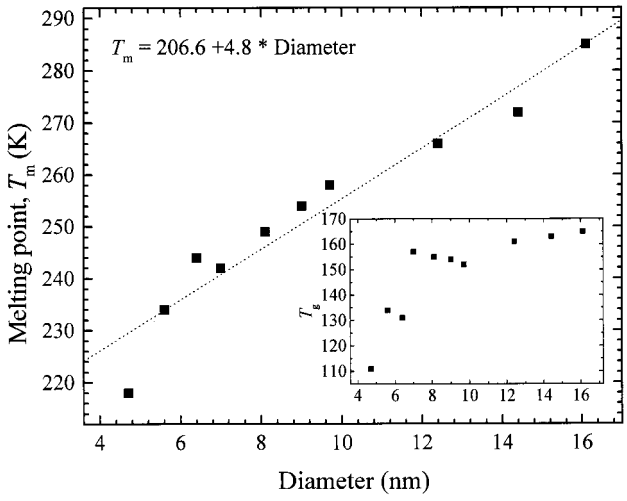

Figure 5. Dependence of the melting point on diameter for PE particles with a chain length of 100 beads. Dashed lines show the least-squares fit (slope = 4.8 K/nm; intercept = 206.6 K). The inset shows dependence of the glass transition temperature.

transition temperature on chain length is attributed to molecular weight and nonbonded energy of each chain.

Figure 5 shows dependence of melting point and glass transition temperature on the diameter of the PE particles. The dramatic reduction of the melting point

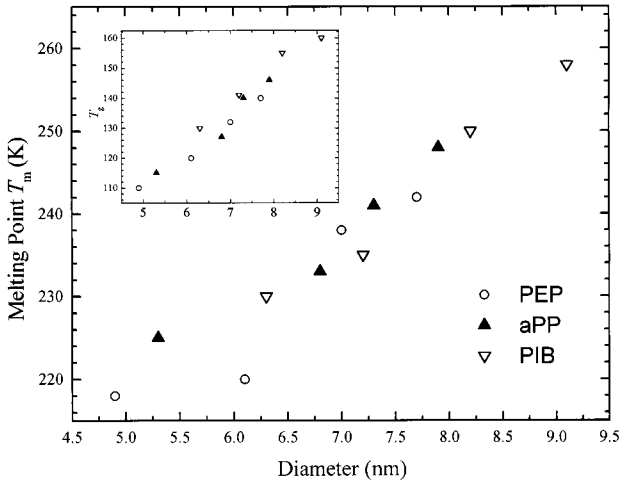

Figure 6. Dependence of the melting point on diameter for PEP, aPP, and PIB particles. The inset shows dependence of the glass transition temperature.

Table 3

no. of backbone atoms	cohesive energy[a] (kcal/mol)	T_m (K)	T_g (K)	C_p (cal/(mol K)) $T \le T_m$	C_p (cal/(mol K)) $T \ge T_m$
Polyethylpropylene (PEP)					
3 000	3 279	218	110	7.80	9.23
6 000	7 014	220	120	7.87	8.89
9 000	11 160	238	132	7.91	9.09
12 000	14 520	242	140	7.99	8.78
Atactic Polypropylene (aPP)					
3 000	3 500	225	115	6.42	6.70
6 000	7 350	233	127	6.33	6.86
9 000	12 920	241	140	6.42	6.80
12 000	16 230	248	146	6.50	6.76
Polyisobutylene (PIB)					
3 000	4 080	230	130	6.21	6.65
6 000	7 880	235	141	6.20	6.51
9 000	12 780	250	155	6.21	6.77
12 000	18 780	258	160	6.24	6.80

[a] The values are calculated from NHC simulations at 10 K.

for the polymer particles is a example of surface effect and shows the importance of size. Since the large ratio of surface atoms to the total number leads to a significant reduction of the nonbonded interactions, the melting point decreases with decrease of the total number of atoms. In the figure, the dot line is obtained with a least-squares fit from 6000 atoms to 120 000 atoms. From the line, the estimated diameter of the particles which may be able to have the bulk melting point (415 K) is around 43 nm. Figure 6 shows dependence of melting point on the diameter of the PEP, aPP, and PIB particles. The behavior of the melting point of the PEP, aPP, and PIB particles is similar to the PE particles. Table 3 summarizes thermal properties of the particles with respect to size.

C. Conformations. The radial distribution function, which provides information on the intra- and intermolecular structure, of the simulated bulk PE was in very good agreement with experimental data. Comparing the bulk system with the nanoscale spherical particles, we can study the conformational changes of the particles due to the size reduction and the shape. Figure 7 shows how the radial distribution function changes from the bulk simulation to that for particles of different sizes. For the amorphous PE particles, the peak positions of the radial distributions are insensitive to the size in the diameter range studied here. The most notable difference is in the amount of gauche conformations as signified by the magnitude of the peak at 3.2 Å. For the smaller particles this peak is almost entirely missing. The larger particles tend to have a somewhat higher concentration of gauche conformations but still significantly less than the bulk. This reduction in the conformational disorder as the diameter of the particle decreases is a surface-induced phenomenon. As the particle diameter decreases, the surface area-to-volume ratio increases, and the polymer chains are forced to lie mostly on the surface of the spherical particle. The surface tends to force the polymer chains to have a much higher percentage of trans configurations. The average end-to-end distance of the surface chains is longer than that of the inner chains, and the inner chains have more gauche configurations than the surface.[6] Figure 8 shows radial distribution functions for the PEP, aPP, and PIB 12 000 backbone atom particles with a chain length of 100 monomers at a temperature of 100 K. As can be seen, the gauche peak around 3.2 Å for the particles are significantly smaller than the bulk systems.

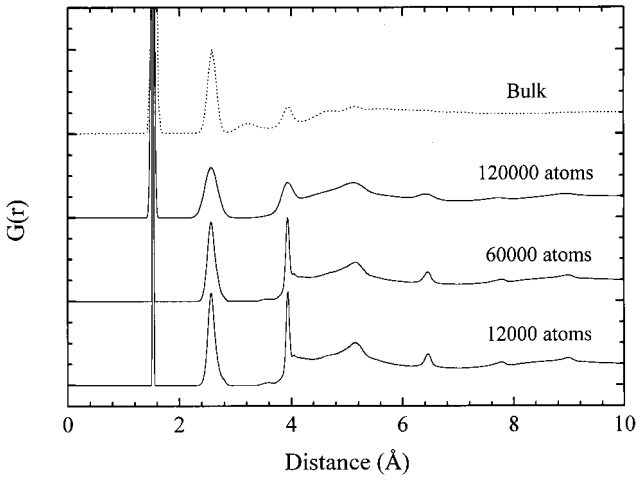

Figure 7. Dependence of the radial distributions on size of a PE particle with a chain length of 100 beads. Those distributions are calculated from NHC constant temperature MD simulations. The three peaks are 1.54, 2.57, and 3.94 Å corresponding to the distance of C_i-C_{i+1}, $C_i\cdots C_{i+2}$, and $C_i\cdots C_{i+3}$ (trans), respectively.

IV. Conclusions

We have used an efficient molecular dynamics method for modeling various nanosize polymer particles and analyzed the characteristics and thermal properties of the particles generated with up to 120 000 atoms. The results show that surface effects provide interesting properties that are different from those of the bulk polymer system. In particular, the melting point and glass transition temperature were found to be dramatically dependent on the size of the polymer particles. Our approach to generate amorphous polymer particles can be used to model various types of polymer particles, and the molecular dynamics simulations used here should provide useful insights to explain and predict the properties and behavior of ultrafine polymer particles to be used in future new materials and devices.

Recently, we have introduced a new method to obtain a complete set of frequencies for the density of states spectrum $g(\omega)$ in a large polymer system with up to 12 000 atoms involving all 36 000 degrees of freedom. Using the density of vibrational states, we investigate thermal properties (heat capacity, entropy, Gibbs free

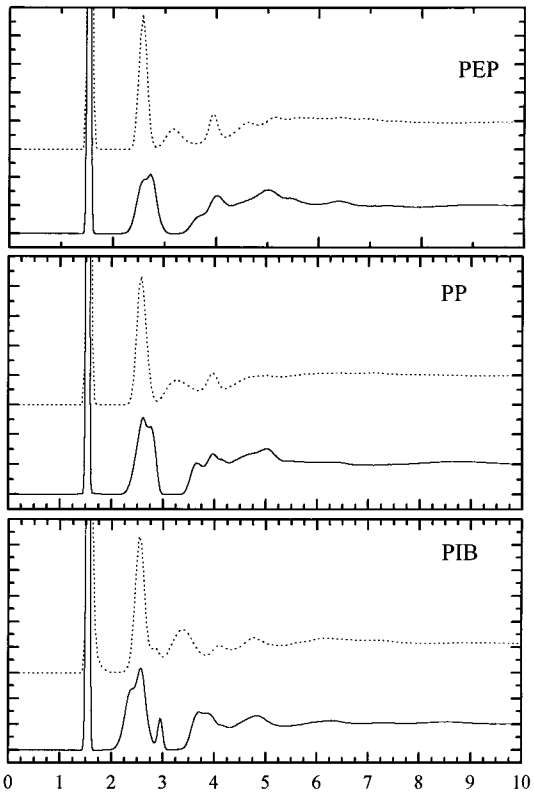

Figure 8. Radial distributions on size of PEP, aPP, and PIB particles with a chain length of 100 beads (solid lines). Those distributions are calculated from NHC constant temperature MD simulations. The dashed lines are obtained from the bulk simulations.

energy, etc.) for the particles.[21,22] Finally, we note that these particles can easily be electrically charged, and semiclassical studies of the electronic properties of these particles have been studied, indicating the possibility for the development of a new generation of quantum dots.[23,24]

Acknowledgment. This research is sponsored by the Division of Materials Sciences, Office of Basic Energy Sciences, U.S. Department of Energy, under Contract DE-AC05-96OR22464 with Lockheed Martin Energy Research Corp. K.F. is supported by the Post-doctoral Research Associates Program administered jointly by Oak Ridge National Laboratory and the Oak Ridge Institute for Science and Education. We are grateful to Professor Kumar and Professor Mattice for many helpful comments.

References and Notes

(1) Kung, C.-Y.; Barnes, M. D.; Sumpter, B. G.; Noid, D. W.; Otaigbe, J. U. *Polym. Prepr. (ACS, Div. Polym. Chem.)* **1998**, *39*, 610.
(2) Barnes, M. D.; Kung, C.-Y.; Lermer, N.; Fukui, K.; Sumpter, B. G.; Noid, D. W. *Opt. Lett.* **1999**, *24*, 121.
(3) Barnes, M. D.; Ng, K. C.; Fukui, K.; Sumpter, B. G.; Noid, D. W. *Macromolecule* **1999**, *32*, 7183.
(4) Ichinose, N.; Ozaki, Y.; Kashu, S. *Superfine Particle Technology*; Springer-Verlag: London, 1992.
(5) Hayashi, C.; Uyeda, R.; Tasaki, A. *Ultra-Fine Particles Technology*; Noyes: Westwood, NJ, 1997.
(6) Fukui, K.; Sumpter, B. G.; Barnes, M. D.; Noid, D. W.; Otaigbe, J. U. *Macromol. Theory Simul.* **1999**, *8*, 38.
(7) Fukui, K.; Sumpter, B. G.; Barnes, M. D.; Noid, D. W. *Comput. Theor. Polym. Sci.* **1999**, *9*, 245.
(8) Fukui, K.; Sumpter, B. G.; Barnes, M. D.; Noid, D. W. *Polym. J.* **1999**, *8*, 664.
(9) Sumpter, B. G.; Noid, D. W.; Wunderlich, B. *J. Chem. Phys.* **1990**, *93*, 6875.
(10) Yan, J.; Boyd, R. H. *J. Chem. Phys.* **1998**, *108*, 9912.
(11) Argon, H. A. S.; Suter, U. W. *Macromolecules* **1993**, *26*, 1097.
(12) Antoniadis, S. J.; Samara, C. T.; Theodorou, D. N. *Macromolecules* **1998**, *31*, 7944.
(13) Neyertz, S.; Brown, D.; Thomas, J. O. *J. Chem. Phys.* **1994**, *101*, 10064.
(14) Han, J.; Boyd, R. H. *Macromolecules* **1994**, *27*, 5365. Pant, P. V. K.; Boyd, R. H. *Macromolecules* **1992**, *26*, 679. Boyd, R. H.; Pant, P. V. K. *Macromolecules* **1991**, *24*, 6325. Boyd, R. H.; Breitling, S. M. *Macromolecules* **1974**, *7*, 855.
(15) Connolly, M. L. *J. Am. Chem. Soc.* **1985**, *107*, 1118.
(16) Dorulker, P.; Mattice, W. L. *Macromolecules* **1998**, *31*, 1418.
(17) Kumar, S. K.; Vacatello, M.; Yoon, D. Y. *J. Chem. Phys.* **1988**, *89*, 5206.
(18) Tanaka, K.; Takahara, A.; Kajiyama, T. *Macromolecules* **1997**, *30*, 6626.
(19) Doucet, J.; Weber, J. *Computer-Aided Molecular Design: Theory and Applications*; Academic Press: San Diego, 1996.
(20) Fukui, K.; Sumpter, B. G.; Barnes, M. D.; Noid, D. W., manuscript in preparation.
(21) Fukui, K.; Sumpter, B. G.; Noid, D. W.; Yang, C.; Tuzun, R. E. *J. Phys. Chem. B* **2000**, *104*, 526.
(22) Fukui, K.; Sumpter, B. G.; Noid, D. W.; Yang, C.; Tuzun, R. E. *J. Polym. Sci., Part B* **2000**, *38*, 1812.
(23) Runge, K.; Sumpter, B. G.; Noid, D. W.; Barnes, M. D. *J. Chem. Phys.* **1999**, *110*, 594.
(24) Runge, K.; Sumpter, B. G.; Noid, D. W.; Barnes, M. D. *Chem. Phys. Lett.* **1999**, *299*, 352.
(25) Karasawa, N.; Dasgupta, S.; Goddard, W. A., III. *J. Phys. Chem.* **1991**, *95*, 2260.

MA000045K